

SPECTRAL IMAGE UTILITY SENSITIVITY TO IMAGE PREPROCESSING AND INFORMATION EXPLOITATION PARAMETERS

Marcus S. Stefanou

United States Air Force
Rochester Institute of Technology
Rochester, New York 14623 USA
Email: mss3679@cis.rit.edu

John P. Kerekes

Rochester Institute of Technology
Chester F. Carlson Center for Imaging Science
54 Lomb Memorial Drive
Rochester, New York 14623 USA

ABSTRACT

For a wide range of application areas, quantifying the ability of a spectral image to satisfy the informational requirements of an application task would be desirable. We propose that this metric may be termed the “image utility” and present a method for assessing the utility of spectral images for the subpixel target detection task. In this paper, we investigate the sensitivity of this utility metric to various image chain parameters. In particular, we examine the effect of small variations of preprocessing and target detection scenario parameters on the assessed utility of a spectral image. We offer a method of quantifying the sensitivity to facilitate a rank ordering of parameter sensitivities. This exploration constitutes an initial step towards gaining a fuller understanding of the key parameters that drive spectral image utility.

Index Terms— spectral image utility, subpixel target detection, sensitivity analysis

1. INTRODUCTION

Improvements in passive electro-optical (hyper- or multi-) spectral imaging offer the potential for enhanced information exploitation in a wide array of application areas. Because many factors impact performance for a particular application, the ability to quantitatively compare performance across different images and various exploitation task scenarios would be beneficial. Toward this end, we have developed an image *utility* metric that consistently quantifies the ability of an image to satisfy application-specific performance measures. Such a metric could then be applied to many images to build a catalog of images covering a range of possible image acquisition and application-specific scenarios. These utility-labeled images could be used to predict the utility of like-parameter images during sensor design trade studies, enable imagery collection planning based on attaining images with the highest possible utility, and form the basis of a searchable image archive.

For the specific task of target detection, image utility depends on a wide array of factors: choice of detection algorithm, method of atmospheric compensation; size, spectral character, and variability of the target; spectral and spatial resolution; and scene spectral complexity. These factors may be categorized into parameters describing scene composition, sensor characteristics, image acquisition conditions, image preprocessing, and information exploitation (target-detection) scenario. In order to

realize the benefits of utility-labeled images, it is necessary to understand the relative role that each parameter plays in calculation of the utility. Knowledge of the utility sensitivity to particular parameters will streamline the development of a robust utility metric by focusing efforts on those parameters having the greatest impact on utility. An appreciation of utility sensitivity to image chain parameters will also help reveal conditions under which the utility metric may fail to accurately characterize the situation, thus adding value to the analyst’s confidence in interpreting the utility metric.

In [1], we introduced a methodology to determine the utility of a spectral image for subpixel target detection applications. This image-derived method differed from other spectral image utility approaches [2-3] in that it did not require prior knowledge of image acquisition parameters, provided a self-contained means to both *assess* and *predict* spectral image utility, and derived required information from a specific image rather than a notional statistical description of the image or sensor characteristics. We calculated utility by sampling the receiver operating characteristic (ROC) curve to obtain a probability of detection associated with a specified false alarm probability (PFA). In this paper, we focus on the assessment of utility and introduce a refined definition of utility that better captures the subtle differences between detection rates at low PFAs. Our goal is to describe the sensitivity of the assessed image utility to image preprocessing and information exploitation parameters, since the image analyst only has control over these two image chain parameters when exploiting an image.

2. APPROACH

2.1. Assessed image utility

The utility of a particular image for detecting a given subpixel target is assessed using a receiver operating characteristic (ROC) curve that expresses the probability of detection over a range of probabilities of false alarm. The probabilities used in the ROC curve are derived from the distributions of the test statistic at the output of the target detection algorithm. While any detector, $D(\cdot)$, may be used to produce a scalar test statistic, we choose the spectral matched filter, represented as the $K \times 1$ filter vector, \mathbf{w} , where K is the number of spectral channels, because of its simplicity and generally robust performance in the subpixel target detection task. The filter vector is constructed using the $K \times K$ image inverse covariance matrix, Σ^{-1} , estimated from the image, and a $K \times 1$ target mean vector, \mathbf{t} , drawn from a spectral library, and the $K \times 1$ image mean vector, $\boldsymbol{\mu}$.

$$\mathbf{w} = \frac{\Sigma^{-1}(\mathbf{t}-\boldsymbol{\mu})}{(\mathbf{t}-\boldsymbol{\mu})^T \Sigma^{-1}(\mathbf{t}-\boldsymbol{\mu})} \quad (1)$$

Traditional approaches to target detection require ground truth and targets in the image with which to calculate a ROC curve. To facilitate the utility assessment of *any* spectral image, we create a binary hypothesis test consisting of a target absent and target present case. The target present case is created by *fractionally implanting* a target spectrum in every spatial pixel of the image as described in [4]. We call this method of assessing image utility for subpixel target detection applications the *target implant method*. The resulting ROC curve is a summary of the overall detectability of the implanted target over the entire image.

A pixel at a given spatial location in the image is represented as the $K \times 1$ vector, \mathbf{x} . We assume that \mathbf{x} and the reference target vector are in reflectance space. We create the target absent case by applying the detector operator, D , to each pixel of the image:

$$y_{TA} = D(\mathbf{x}) \quad (2)$$

The scalar y_{TA} is the output in the target absent case at one pixel location. The target present case is created by applying the detector to each pixel location of the original image in which the $K \times 1$ target vector has been implanted, resulting in the scalar output y_{TP} :

$$y_{TP} = D(\mathbf{x}_{TP}) \quad (3)$$

The implantation of the target is accomplished in a fractional manner using the prescribed subpixel fraction f in each pixel of the image as:

$$\mathbf{x}_{TP} = f\mathbf{t} + (1-f)\mathbf{x} \quad (4)$$

The $K \times 1$ implanted target pixel vector \mathbf{x}_{TP} is created by first realizing a $K \times 1$ random vector \mathbf{t} from a normal random process described by the statistical parameters of the $K \times 1$ target mean vector, \mathbf{t} , and $K \times K$ covariance matrix, Σ_T . These parameters are drawn from a reference library created by careful collection of known target pixel vectors from the HYperspectral Digital Imagery Collection Experiment (HYDICE) imagery [5]. The random target vector \mathbf{t} is then mixed *fractionally* with every data pixel to the specified subpixel mixing fraction f .

The target absent and present probability density functions are estimated from the detector output histograms for the entire image and integrated at all detection threshold settings to generate the probability of false alarm (PFA) and probability of detection (PD), which lead to the ROC curve.

In order to produce a scalar metric that conveys the shape of the ROC curve, we employ the area under a ROC curve over a PFA interval of interest. The area under curve (AUC) is a figure of merit for detection performance from medical diagnostics. In target detection for spectral images, the operational range of PFA will tend to be rather low, since typically only a small number of false alarms are acceptable. In order to better represent this desire to operate at low PFAs, we apply a weighting function $z(PFA)$, to the calculation of the AUC. A simple weighting function is a rectangular window that applies equal weight to all PFAs in a desired operating range (from the lowest achievable PFA to the specified PFA) and zero elsewhere. Any weighting function may be applied to meet the specific requirements of the particular target detection scenario, offering great flexibility. The integral version of the AUC is represented as:

$$AUC(\mathbf{t}, f, D(\mathbf{x}), PFA) = \frac{\int_0^1 z(PFA) \cdot PD(\mathbf{t}, f, D(\mathbf{x}), PFA) dPFA}{\int_0^1 z(PFA) dPFA} \quad (5)$$

Note that the AUC is a function of the target type, implant fraction, detector, and PFA by virtue of PD dependence on these factors. In practice, a discrete approximation to this integral is calculated. The AUC is normalized by the AUC associated with a perfect detection situation (modulated by the window function). This has the effect of transforming the AUC into a utility metric between 0 and 1, allowing us to readily compare image utilities.

2.2. Parameters of interest and baseline situation

We pursue the empirical exploration of utility sensitivity by selecting specific preprocessing and target detection scenario parameters from a range of possible settings and noting the resulting image utilities for each parameter combination. The image preprocessing parameters investigated are the gain and offset used in the empirical line method (ELM) of atmospheric compensation and the spectral range. The target detection scenario parameters are the target implant physical target size (subpixel mixing fraction) and the specified PFA. These are just four parameters among a large number of options, and we investigate these because they are readily quantifiable as the independent variables upon which the utility depends. Preprocessing parameters not investigated in this paper are: alternative atmospheric compensation methods, optimal band selection, and handling of bad retrieved reflectances. Target detection scenario parameters not considered are target variability and detector type.

Fig. 1 shows the image used for this analysis. It is a synthetic hyperspectral image generated using the Digital Imaging and Remote Sensing Image Generation (DIRSIG) model. The sensor has HYDICE characteristics (210 channels with 10 nm resolution covering 400 – 2500 nm spectral range). DIRSIG is a physics-based approach to synthetic image generation, and it lends itself well to exploration of image chain parameters, particularly those sensor parameters that need to be varied independently [6]. The ground resolved distance (GRD) of the image is 4 m and signal-to-noise ratio is 100.

The baseline situation is a reflectance image obtained using standard ELM, working only with the 145 channels not impacted by atmospheric absorption, using two targets green camouflage tent (c6) and green nylon (f4) of 1 m linear dimension (fractional implant of 0.0625) at a specified PFA of 5×10^{-4} .

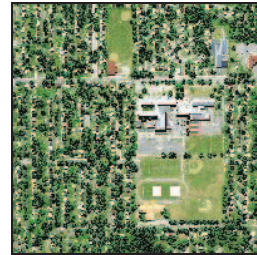


Fig. 1. DIRSIG Image Used for the Sensitivity Analysis

2.3. Method for calculating utility sensitivity

Our approach to exploring the sensitivity is to choose a baseline scenario and then vary the parameters in question about the baseline over a reasonable range, calculating the utility for each parameter combination. The parameters for the ELM gain and offset are varied from their original state by multiplying them independently with a scalar factor between 1 and 2 in 10 evenly spaced increments. This simulates the effect of a suboptimal ELM resulting in a gain or offset that is different than the “good” gain and offset used to obtain the reflectance image. The spectral range is altered from the baseline by computing the utility at upper limits of 750, 1000, 1500, and 1700 nm. This simulates the cutoff wavelengths of different detector array technologies or the analysts’ desire to use only a subset of available channels. Target size is investigated by varying the target implant fraction from 1 to 100% in ten increments. The specified PFA is varied in ten increments from 1×10^{-5} to 1×10^{-4} . The specified PFA is an important operational parameter that is determined by the specific needs of the image analysis task in terms of the acceptable number of false alarms.

The utility sensitivity is calculated using the plots of utility versus each of these parameters over the range of parameter variation. The quantification of utility sensitivity is simple. We calculate the slope using three points in the middle of the range of parameters. This is an approximation to the partial derivative representing the change in utility with respect to the change in the parameter. In order to allow equitable comparison of the slopes, we normalize the parameter axis relative to the maximum value attained. We also use the absolute value of the slope, since we are not concerned as much with the direction of utility change as the magnitude of the change. We adopt this straightforward approach in an attempt to gain traction on an otherwise very complicated situation.

3. RESULTS

We show plots of utility versus the parameter being varied for four of the parameters to give a quantitative sense for their general behavior. The ELM parameters shown in Fig. 2 reveal that this particular image and c6 target detection situation responds more strongly to increases in the scaling of the offset term of the ELM than the gain term. The ELM offset term is compensating for the upwelled radiance, and a larger offset term has the effect of significantly decreasing the reflectance in the first twenty channels. This creates an increasingly difficult detection situation, and pulls the overall utility down as Fig. 2 shows.

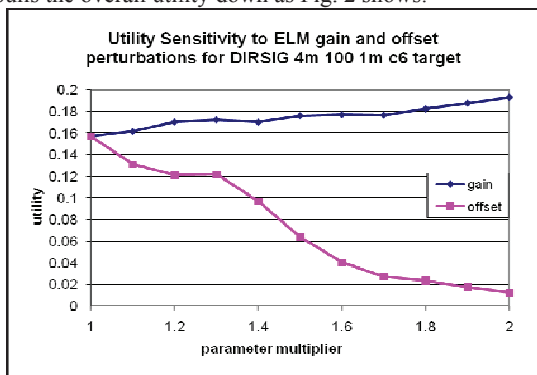


Fig. 2. Utility versus ELM parameters

The ELM gain scaling increase creates a much smaller reflectance, and therefore, relative to this target, makes the detection slightly easier. While not shown, target f4 shows no change in utility (stays at a constant utility of 1 since it is a very easy target to detect in this image) as the ELM parameter is changed.

Fig. 3 shows an increasing trend in utility with the upper limit of spectral range, as we expect more spectral characteristic features available in other parts of the Vis/NIR to contribute favorably to detection. The two targets show an increase in utility, but the f4 target is more detectable when spectral features beyond 1000 nm are included.

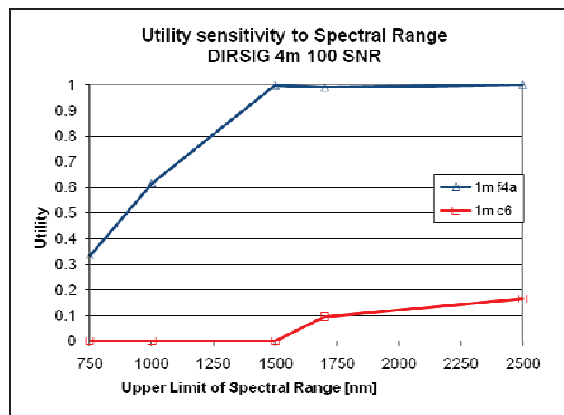


Fig. 3. Utility versus Spectral Range

Fig. 4 shows the behavior of utility with target size, which is the product of the GRD and the square root of the target implant fraction, assuming that we have a square target and square pixels. The increase in utility as target size increases from 0.4 to 0.8m is significant for the f4 target, whereas it is more gradual for the c6 target. Both reach have a final utility of 1 for full pixel targets, but

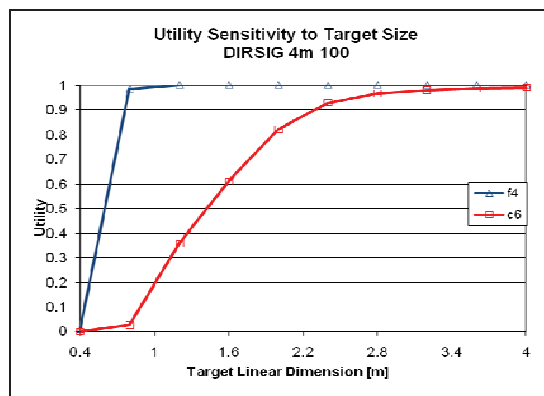


Fig. 4. Utility versus Target Size

the f4 target, attains the perfect utility by a 1.2m target size, due to its much more detectable nature in this image.

Fig. 5 illustrates the role of the specified PFA on the utility. The specified PFA is the limit over which the area under the ROC curve is calculated, so a smaller PFA means that the role of the early false alarms becomes very important in determining the shape of the ROC curve and subsequent utility. A larger specified

PFA means that more correct detections are accrued before the threshold

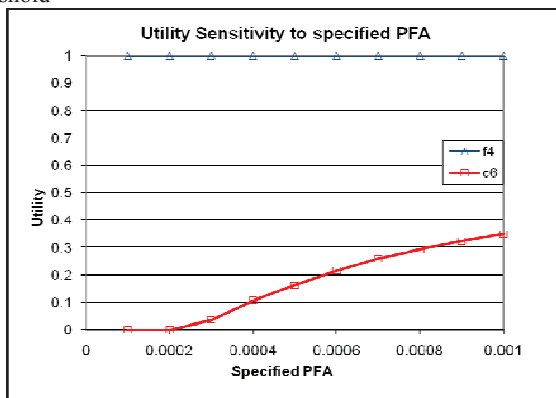


Fig. 5. Utility versus specified PFA

associated with the specified PFA is reached, thus contributing to a significantly larger area under the ROC curve. We see again that because target f4 is such an easy detection, the utility is insensitive to the specified PFA. The c6 target displays significant sensitivity to the specified PFA since the detection scenario is more difficult.

One observation for all of these plots is that the specific operating point defined by the target type, fraction, and detector will make a difference in terms of the utility sensitivity. This is exactly what makes the utility sensitivity challenging to pin down, because the sensitivity for a particular target/image combination will vary. It is with this note of caution that we approach the relative ranking of the parameters according to sensitivity calculated using the slope of the utility versus parameter plots. Table 1 shows the rankings associated with the c6 and f4 targets in the image. The sensitivity value was obtained by averaging the sensitivity resulting from each target type.

Rank	Sensitivity	Parameter	Image Chain Category
1	0.86	spectral range	preprocessing
2	0.80	target size	target detection scenario
3	0.28	ELM offset	preprocessing
4	0.27	specified PFA	target detection scenario
5	0.03	ELM gain	preprocessing

Table 1: Utility Sensitivity Parameter Ranking

While this table by no means suggests that every image, or even every target in this image, will show similar rankings of sensitivity, it is an initial attempt to show that quantifying of the effects of varying image chain parameters on image utility is viable and informative.

4. SUMMARY AND DISCUSSION

This paper has proposed a metric for image utility based on subpixel target detection performance in the hypothetical scenario of a target implanted in every image pixel. The behavior of this utility metric was investigated by varying image preprocessing and target detection scenario parameters and capturing the resultant changes in utility. The utility sensitivity was defined as the instantaneous slope about a midpoint in the normalized parameter range. The utility sensitivity to five parameters of the image chain

was calculated using this approach and a rank ordering of the parameters for this specific image and target was compiled.

While the general behavior of the utility with respect to the parameter variation confirmed intuition, there were no expectations as to how the parameters might be ranked. This turns out to be dependent not only on the specific image and target in question, but also on the method of interpreting the parameter variation, the choice of range to use in varying the parameters, and the part of the curve used for the slope calculation. A more rigorous approach in which more parameters for several images are compared as fairly as possible would be a logical next research direction.

This research suggests that there is much room for further investigation. We have established a foundation with which to quantify image utility and begin to understand the sensitivity of that utility to various image chain parameters. Further building on this foundation is required to realize the full potential of such a utility metric.

5. REFERENCES

- [1] M. S. Stefanou and J. P. Kerekes, "Spectral Image Utility Prediction," *Proceedings of International Geoscience and Remote Sensing Symposium 2007*, IEEE, Barcelona, Spain, July 2007.
- [2] S. Shen, "Spectral quality equation relating collection parameters to object/anomaly detection performance," *SPIE Proceedings on Algorithms and Technologies for Multispectral, Hyperspectral, and Ultraspectral Imagery IX*, vol. 5093, pp. 29-36, 2003.
- [3] J. P. Kerekes and S. M. Hsu, "Spectral quality metrics for VNIR and SWIR hyperspectral imagery," *Proceedings of SPIE on Algorithms and Technologies for Multispectral, Hyperspectral, and Ultraspectral Imagery X*, vol. 5425, pp. 549-557, 2004.
- [4] C. Cafer, M. Stefanou, E. Nielsen, A. Rizzuto, O. Raviv, and S. Rotman, "Analysis of false alarm distributions in the development and evaluation of hyperspectral point target detection algorithms," *Optical Engineering*, vol. 46, no. 7, pp. 076402-1-15, July 2007.
- [5] J. P. Kerekes and J. E. Baum, "Spectral Imaging System Analytical Model for Subpixel Object Detection," *IEEE Trans. On Geosci. and Rem. Sens.*, vol. 40, no. 5, pp. 1088-1101, May 2002.
- [6] Schott, J.R., Brown, S. D., Raqueno, R. V., Gross, H. N., and Robinson, G., "An Advanced Synthetic Image Generation Model and Its Application to Multi/Hyperspectral Algorithm Development", *Canadian Journal of Remote Sensing*, Vol. 25, No. 2, June 1999.

DISCLAIMER

The views expressed in this article are those of the authors and do not reflect the official policy or position of the United States Air Force, Department of Defense, or the U.S. Government.